NACA RM E53E22

NACA

RESEARCH MEMORANDUM

BURNING RATES OF SINGLE FUEL DROPS AND THEIR APPLICATION TO TURBOJET COMBUSTION PROCESS

By Charles C. Graves

Lewis Flight Propulsion Laboratory
Cleveland, Ohio

NATIONAL ADVISORY COMMITTEE
FOR AERONAUTICS
WASHINGTON

July 16, 1953
Declassified December 12, 1954

NATIONAL ADVISORY COMMITTEE FOR AERONAUTICS

RESEARCH MEMORANDUM

BURNING RATES OF SINGLE FUEL DROPS AND THEIR APPLICATION TO TURBOJET COMBUSTION PROCESS

By Charles C. Graves

SUMMARY

Burning rates were determined for single isooctane drops suspended in various quiescent oxygen-nitrogen atmospheres at room temperature and pressure. The burning rates were compared with those predicted by a previously developed theory based on a heat- and mass-transfer mechanism and with values predicted by a modification to this theory. The drop-burning-rate data were applied to equations for a burning fuel spray in order to calculate the predicted change in burning rate of a fuel spray with variation in oxygen concentration. The results so obtained were compared with the change in combustion efficiency of a single turbojet combustor with inlet oxygen concentration, as determined in a previous investigation.

The drop burning rates were proportional to drop diameter and increased approximately 34 percent when oxygen concentration of the surrounding oxygen-nitrogen atmosphere was raised from 17.0 to 34.9 percent by volume. The experimentally determined burning rates agreed well with those predicted by the modified heat- and mass-transfer theory. The predicted change in combustion efficiency with inlet oxygen concentration was appreciably smaller than that observed in the combustor tests.

INTRODUCTION

Operational experience with turbojet and ram-jet engines has shown that combustion efficiency is adversely affected by increase in flight altitude. The establishment of design criteria to improve combustion efficiency at altitude is one of the most important problems confronting the combustion-chamber designer. One phase of combustion research being conducted at the NACA Lewis laboratory is concerned with the relative importance of such component processes as fuel-spray vaporization, mixing, ignition, and reaction in the determination of combustion efficiency. In a recent investigation (ref. 1), an attempt was made to relate the changes in combustion efficiency of a J33 single combustor, operating with liquid isooctane, to a particular component process. The effects of fuel-flow rate, inlet pressure, and inlet oxygen concentration on combustion efficiency were determined for the conditions of

constant temperature and weight flow rate of the inlet oxygen-nitrogen mixture. At a given fuel-flow rate, the combined effects of inlet pressure and inlet oxygen concentration on combustion efficiency were correlated in terms of (a) selected fundamental combustion properties of isooctane and (b) a simplified reaction-kinetics equation. The results indicated that changes associated with the kinetics of the gas phase might explain the observed trends.

The correlations obtained in reference 1 were based on the assumption that the fraction of combustor volume required for the fuel-spray evaporation and mixing steps was either constant with variation in inlet conditions or negligibly small. In reference 2, an attempt was made to determine the importance of the fuel-spray evaporation step on the correlations of reference 1. Similar data were obtained with the same combustor (but with a different fuel-injection system); the fuel-spray evaporation step was eliminated by the use of a gaseous fuel, propane. The relative effects of combustor-inlet pressure and oxygen concentration on combustion efficiency were found to be approximately the same for either the gaseous or the liquid fuel. However, the general level of combustion efficiency attained with gaseous propane was appreciably higher than that attained with liquid isooctane. While such differences in performance level cannot be definitely attributed to a particular process, one of the obvious explanations would be the fuel-evaporation step.

The purpose of the investigation reported herein was to study the role of the fuel evaporation step in determining the changes in combustion efficiency with inlet oxygen concentration observed in reference 1. The investigation was limited to a special case of evaporation (burning fuel spray) in which the heat required for vaporization is supplied from burning zones surrounding individual fuel drops. In order to predict changes in burning rate of the entire fuel spray, an extension to the theoretical relations of Probert (ref. 3) was derived for the case of a fuel spray burning in a duct where heat release changes local velocity and, hence, residence time. These relations were based on the simplifying assumption that the burning rate of the entire spray was a function of experimentally determined burning rates of the individual drops. In references 4 and 5, relations were derived which predict the effect of oxygen concentration on burning rates of single drops; however, no experimental data were available to verify the theory. Accordingly, burning rates were determined for single drops of isooctane suspended in various quiescent oxygen-nitrogen atmospheres at room temperature and pressure. The data obtained were compared with values predicted by the theory of reference 5 and with values predicted by a modification of this theory which is presented herein. The drop-burning-rate data were also used in conjunction with the theoretical relations for the burning fuel spray in order to predict the change in combustion efficiency with inlet oxygen concentration. The predicted changes in combustion efficiency were compared with those observed in reference 1.

APPARATUS AND PROCEDURE

The apparatus and procedure used in determining the burning rate of single isooctane drops in various quiescent oxygen-nitrogen mixtures were similar to those described in reference 6. Isooctane drops approximately 1700 microns in diameter were suspended from a quartz filament, ignited, and photographed while burning. The burning rate, defined as the time rate of change in drop weight, was determined from measurements of the change in drop diameter with time. A schematic sketch of the apparatus is presented in figure 1. The filament and the ignition source were mounted in a chamber having inside dimensions of 12 by 12 by 18 inches.

Filament. - The filament, approximately 180 microns in diameter, was drawn from a 5-millimeter quartz rod. To reduce possible effects of the rod on the drop burning rate, the filament was drawn to a length of approximately $2\frac{1}{2}$ inches and bent at right angles 1 inch from the tip (fig. 1). Since the surface tension of isooctane is low (approx. 22 dynes/cm at room temperature), the tip was slightly enlarged to permit the suspension of large drops. A fine pipette, drawn from pyrex tubing, was used to suspend the drops from the filament.

Ignition source. - The drop was ignited by means of a small ethylene diffusion flame, which could be moved in a vertical plane past the underside of the drop. Oscillations of the drop caused by the passage of the ignition flame hindered accurate measurement of drop diameter during the first portion (approx. 1/8 sec) of burning. Provided the ignition flame was small, drop distortion did not severely affect measurements during the initial burning period.

Background illumination. - A silhouette of the drop was obtained by providing strong background illumination which offset the luminosity of the flame. This illumination consisted of a focusing spot lamp mounted behind a ground-glass plate.

Photographic system. - The photographic system consisted of a $5\frac{1}{4}$-inch focal length, f/4.5 lens and a 16-millimeter camera (without lens). The lens was mounted approximately $6\frac{1}{2}$ inches from the drop. This produced an image on the film that was approximately four times the drop size. The camera was operated by a 110-volt synchronous motor which gave a constant speed of 24 frames per second.

Oxygen-nitrogen-mixture control. - Prior to each series of runs, the chamber was purged with the appropriate oxygen-nitrogen mixture. To facilitate purging, the chamber was fitted with a horizontal partition which was lowered prior to purging and gradually raised as the

oxygen-nitrogen mixture was introduced to the chamber. The oxygen-nitrogen mixture was supplied through a pressure regulator to the bottom of the chamber. The chamber pressure was maintained slightly above atmospheric pressure during purging. Since a negligible fraction of the oxygen in the chamber was consumed during the burning of a single fuel drop, it was possible to obtain several points for each purging of the chamber. Orsat analysis at the end of a series of runs indicated a negligible change in oxygen concentration.

Photograph analysis. - A typical set of photographs of the silhouette of a burning drop of isooctane is presented in figure 2. The time interval between successive pictures is 0.125 second.

In order to convert image distances to known distances, a platinum wire having a diameter of 640 microns was positioned in the plane of the filament and photographed at the end of each series of runs.

Kodak super XX film developed in fine-grain developer was found to give satisfactory results. Drop diameters were measured in two planes, each inclined 45° from the vertical. The average of these two measurements was taken as the diameter of an equivalent spherical drop. Distortion of the drop and increasing relative importance of the filament precluded measurements of drop diameters smaller than approximately 700 microns.

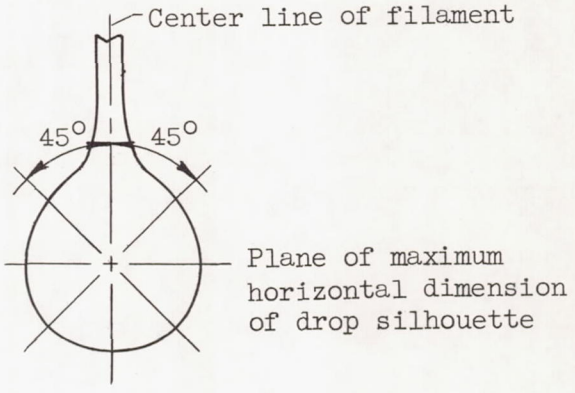

RESULTS AND DISCUSSION

Data presented in reference 6, indicate that the burning rate of small fuel drops suspended in quiescent atmospheres is proportional to drop diameter. For this condition (see appendix B), the relation between drop diameter and time is given by

$$d_A^2 = d_{A_0}^2 - \beta t \qquad (B8)$$

where d_A is the drop diameter after a burning time t, and d_{A_0} is the drop diameter at time $t = 0$. The constant β is known as the evaporation constant (ref. 3).

In figure 3, plots of the square of the drop diameter against time are presented for isooctane drops burning in quiescent oxygen-nitrogen atmospheres containing 17.0 and 34.9 percent oxygen by volume. The points during burning follow a straight-line relation and satisfy equation (B8). Values of the evaporation constant β are obtained from the slopes of the lines in figure 3. Table I presents values of the evaporation constant, obtained in this manner, for single isooctane drops burning in various quiescent oxygen-nitrogen atmospheres [17.0, 20.9 (air), 24.9, and 34.9 volume percent oxygen] at room temperature and pressure. Arithmetic mean values of the evaporation constant at each oxygen concentration are also presented. The average deviation is 2.4 percent; the maximum deviation, 5 percent. When oxygen concentration was increased from 17.0 to 34.9 percent by volume, the mean value of the evaporation constant increased by 34 percent.

It is of interest to note that the mean value of the evaporation constant in air was approximately 22 percent higher than that reported in reference 6 for isooctane drops burning in still air. No reasonable explanation for this difference was evident.

Comparison of Experimental and Predicted Values of Evaporation Constant

A theoretical treatment of the burning of small fuel drops is given in reference 5. The drop was considered to be separated from a burning zone of negligible thickness by a stagnant film; another stagnant film was assumed to exist between the burning zone and the surrounding atmosphere. Equations were derived for heat transfer in both films and for diffusion of oxygen in the outer film. Relations were obtained for the burning of small fuel drops or solid particles where the film thickness between the burning zone and the surrounding atmosphere was considered infinite, corresponding to a Nusselt number of 2 for heat transfer.

The relations presented in reference 5 were based on the assumption that no dissociation of combustion products occurred. Estimates suggested that correction for dissociation of combustion products would result in but a small change in calculated burning rates of liquid fuel drops. As indicated in reference 5, correction for dissociation effects requires consideration of the relative diffusion rates of the various dissociated products, material balance, equilibrium relations, and heat balance. For hydrocarbon fuels where there is a relatively large number of dissociated products, the determination of dissociation effects becomes quite complex, particularly if the analysis considers the

temperature variations of thermal conductivity, diffusion coefficients, and specific heats. In appendix B, a simplified approach to the problem of dissociation is made for the case of variable thermal conductivity. This approach requires the assumption that the relative proportions of the elements carbon, hydrogen, oxygen, and nitrogen, regardless of their state of chemical combination, remain constant throughout the region between the burning zone and the surrounding atmosphere. The relative proportions of dissociated products in this region then become a function only of temperature. Material- and heat-balance equations are satisfied for this region, but no correction is made for the difference in diffusion rates of the various dissociated products such as that presented in reference 5 for a burning carbon particle. The equations in appendix B have the same general form as those given in reference 5 and are presented primarily to clarify the assumptions required in the calculation of burning rates for the present investigation.

In figure 4, the theoretical and experimental values of evaporation constant are plotted against oxygen concentration in the surrounding oxygen-nitrogen atmosphere. The experimental curve A was drawn using the arithmetic mean values of evaporation constant presented in table I. Curve B gives the theoretical evaporation constant obtained by using the theoretical relations presented in appendix B. The deviation of the theoretical from the experimental curve varies from approximately -4 percent at 17 percent oxygen to approximately -5 percent at 34.9 percent oxygen. While such close agreement between the theoretical and experimental curves is considered fortuitous in view of the assumptions involved in the analysis and the uncertainties in the values of properties used, the results are encouraging. Curve C gives the predicted value of evaporation constant using the assumptions of reference 5. The deviation of the theoretical from the experimental curve varies from -39 percent at 17 percent oxygen to -34 percent at 34.9 percent oxygen.

The principal differences involved in the calculations of curves B and C are: (1) correction for effect of dissociation of combustion products on calculated burning rates, and (2) choice of thermal conductivity values used for the region between the drop surface and the burning zone. In curve C, the thermal conductivity of air was used in this region, whereas curve B was calculated by using estimated values of the thermal conductivity of isooctane vapor. In order to determine the effect of thermal conductivity on the predicted evaporation constant, curve D was calculated using the thermal conductivity of isooctane vapor, but the corrections for dissociation of products described in appendix B were neglected. It is seen that the use of thermal conductivity of isooctane vapor instead of air resulted in an appreciable increase in the calculated evaporation constant. From comparison of curves B and D, it is also observed that the correction for dissociation of combustion products (appendix B) results in a significant decrease in calculated evaporation constant at the higher oxygen concentrations. At the lower oxygen concentrations the effect is small, as was noted in reference 5.

At the high temperatures reached near the burning zone, pyrolysis of the fuel vapor would be extensive. This pyrolysis would result in higher thermal conductivities and, hence, higher calculated evaporation constants. However, the effect is opposed by the higher heat contents of the cracked constituents.

Application of Drop-Burning-Rate Data to Combustor Tests

In reference 1, the combustion efficiency of a J33 single combustor operating with liquid isooctane was determined over a range of inlet oxygen concentrations, inlet pressures, and fuel-flow rates. Some typical data are plotted in figure 5, which presents a plot of combustion efficiency against inlet oxygen concentration for two fuel-flow rates and two inlet pressures. The inlet temperature and the weight-flow rate of the oxygen-nitrogen mixture were held constant at 40° F and 1.0 pound per second, respectively. It is observed that combustion efficiency increased noticeably with increase in fuel-flow rate over the entire range of conditions investigated. It is also noted that the change in combustion efficiency with both inlet pressure and oxygen concentrations is quite pronounced at the lower values of combustion efficiency. In the following section, the data of figure 5 will be treated in terms of an idealized burning fuel spray. The single-drop burning-rate data will be used in conjunction with theoretical relations for a burning fuel spray in order to predict the effect of inlet oxygen concentration on combustion efficiency.

In reference 3, theoretical relations for a burning fuel spray were derived for the following conditions: (1) burning rates of the individual drops are proportional to the drop diameter, (2) the evaporation constant is the same for all drops, (3) all drops have the same available burning time, and (4) the fuel-spray drop-size distribution can be expressed by a Rosin-Rammler distribution function. In appendix C, the relations are extended to the case of a fuel spray burning in a duct where the heat release changes the average velocity along the duct. Values of the drop-size-distribution constants $\bar{x}$ and n of the Rosin-Rammler distribution function were obtained from the data of Bowes and Joyce (ref. 7). No correction was made for the effect of change in properties of isooctane compared with those of the molten wax (simulating kerosene) used in reference 7. The values obtained were considered only as giving an approximate indication of the drop-size distribution for the conditions of figure 5.

In figure 6, the theoretical combustion efficiency of a burning fuel spray, as obtained from the relations of appendix C, is plotted against the parameter $\beta L_{eq}/V_r$ for the two fuel-flow rates of figure 5. Here β is the evaporation constant in square microns per second; L_{eq} is an equivalent combustor length, constant for a given combustor; and V_r is the inlet velocity.

The predicted and experimental changes in combustion efficiency with variation in inlet oxygen concentration are compared in figure 7. The experimental curves are those of figure 5. The predicted curves were obtained by using the curves of figure 6 and the arithmetic mean values of the evaporation constant at the various oxygen concentrations presented in table I. Since the combustor data were obtained at pressures other than atmospheric, it was assumed that the percent change in β with oxygen concentration was the same for all pressures. This assumption is in agreement with the predictions of reference 5 and appendix B. Inlet oxygen concentration had a negligible effect on inlet density and, hence, inlet velocity. Accordingly, for the conditions of constant temperature, pressure, and weight-flow rate of the inlet oxygen-nitrogen mixture, the term L_{eq}/V_r, a measure of residence time based on inlet conditions, could be considered constant. In order to compare the relative change in the predicted and experimental values of combustion efficiency, arbitrary values were assigned to the term L_{eq}/V_r to make the experimental and the predicted curves coincide at low values of oxygen concentration within the ranges covered in the drop-burning and combustor tests. It is observed that the predicted change in combustion efficiency with oxygen concentration is much too small to explain the changes observed in the J33 combustor.

It is also to be noted that the pronounced changes in combustion efficiency with varying inlet pressure as shown in figure 5 cannot be explained in terms of the burning fuel spray. In a recent publication (ref. 8), the burning rates of single fuel drops, determined over a range of pressures from 1 to 20 atmospheres, are reported as being approximately proportional to the fourth root of the total pressure. Accordingly, use of these data in the relations for the burning fuel spray (fig. 6) would also result in an appreciably smaller predicted change in combustion efficiency with variations in inlet pressure than was observed in the combustor tests.

Treatment of combustor data in terms of the burning fuel spray such as has been presented, necessarily involved a number of simplifying assumptions. A number of factors should be considered in transferring single-drop data to the conditions of the combustion-reaction zone: Combustor conditions include (1) higher temperature level, (2) forced convection by drops, (3) local over-rich fuel-oxygen ratios, (4) deposition of part of the spray on combustor walls, (5) errors involved in the use of drop-size distribution data of reference 7, (obtained for nozzle spraying into quiescent atmosphere), and (6) radiation. A detailed discussion of all these factors is beyond the scope of this paper. However, factors 1 to 4 are discussed to some extent in references 4 and 5. Preliminary consideration of these factors indicates that, while some may appreciably affect the absolute burning rate of the spray, their effect on the calculated change in burning rate with oxygen concentration is minor compared with the large differences between predicted and experimental curves shown in figure 7.

It also appears that correction for factors 5 and 6 would not appreciably affect the predicted results. Since the small predicted change in combustion efficiency with oxygen concentration was primarily due to the small change in the evaporation constant, correction for errors in drop-size-distribution data would be small. Appreciable changes in combustion efficiency occurred at the lower oxygen concentrations and under nonluminous flame conditions in which the principal radiation is associated with carbon dioxide and water vapor. Since isooctane drops in the size range expected for the fuel-flow rates of figure 5 are relatively transparent to this radiation, the heat absorbed by the fuel spray from radiation was but a small fraction (less than 5 percent) of the latent heat of vaporization. Accordingly, correction for radiation effects would have resulted in but a small change in predicted results over the range of conditions in which large changes in combustion efficiency occurred.

In view of the complexity of the over-all combustion process, it is possible that the change in combustion efficiency with oxygen concentration and pressure (fig. 5) might be explained in terms of change in burning rate of the fuel spray if proper account were taken of the first four of the aforementioned factors; however, this does not appear likely. It is suggested that some other process involving the chemistry of the reaction might better explain the trends observed in figure 5. It is noted that in reference 1 the combined effects of inlet pressure and oxygen concentrations on combustion efficiency were related to fundamental combustion properties of isooctane and to a simplified reaction-kinetics equation. It is also emphasized that the results of the present investigation do not preclude large possible effects of the fuel-evaporation step on factors not considered, for example, ignition.

Finally, it is noted that the results of the present investigation apply only to the particular experimental conditions of reference 1, under which a fully developed fuel spray having a relatively small mean drop size would be expected. As indicated in references 9 and 10, there are ranges of operation of turbojet combustors where the fuel-atomization and fuel-evaporation steps do exert a significant influence on combustion efficiency, either directly or indirectly.

SUMMARY OF RESULTS

The following results were obtained from an investigation of the burning rates of single isooctane drops in quiescent oxygen-nitrogen atmospheres at room temperature and pressure and from comparison of these data with turbojet-combustor data obtained in a previous investigation:

1. Drop burning rates were proportional to drop diameter and increased approximately 34 percent when oxygen concentration of the surrounding oxygen-nitrogen atmosphere was raised from 17.0 to 34.9 percent by volume.

2. Drop burning rates predicted by a heat- and mass-transfer theory incorporating modifications to a previously developed theory agreed well with the experimentally determined burning rates.

3. Predicted changes in turbojet combustion efficiency with inlet oxygen concentration, based on burning rates of single drops and theoretical relations for a burning fuel spray, were appreciably smaller than the changes experimentally determined in a previous investigation.

Lewis Flight Propulsion Laboratory
National Advisory Committee for Aeronautics
Cleveland, Ohio, April 24, 1953

APPENDIX A

SYMBOLS FOR APPENDIX B

The following symbols are used in appendix B:

D_{O_2}	diffusion coefficient of oxygen, sq ft/sec
d	diameter, ft
ΔH	sensible heat change of unit quantity of fuel when raised to boiling point from temperature existing prior to burning, Btu/lb fuel
h	enthalpy referred to unit quantity of fuel, Btu/lb fuel
h_{O_2}	enthalpy of oxygen referred to unit quantity of fuel, Btu/lb fuel
k	thermal conductivity, Btu/(sq ft)(sec)($^{\circ}$F/ft)
L	latent heat of vaporization of fuel at boiling point, Btu/lb fuel
M_{O_2}	molecular weight of oxygen
Q	heat of combustion of fuel at temperature of surrounding atmosphere, Btu/lb fuel
r_{O_2}	pounds of oxygen required to burn 1 lb of fuel (from stoichiometric equation)
T	temperature, $^{\circ}$F
t	time, sec
W_l	weight of fuel drop, lb
α	volume percent oxygen
β	evaporation constant, sq ft/sec
ρ	density, moles/cu ft
ρ_l	fuel density at mean drop temperature, lb/cu ft
$\frac{d W_l}{dt}$	drop durning rate, lb/sec

Subscripts:

A	drop surface
AB	region between drop surface and burning zone
B	burning zone
BC	region between burning zone and surrounding atmosphere
C	surrounding atmosphere
f	fuel vapor
p	products of combustion

APPENDIX B

PREDICTED EVAPORATION CONSTANT FOR BURNING FUEL DROPS

Stagnant films are considered to exist between a burning zone of negligible thickness and both the drop surface and the surrounding atmosphere. The concentration of oxygen is assumed to be negligible at the burning zone. With the exception of a thin layer at the surface (considered to be at the boiling point of the fuel) the drop temperature is assumed to be at the temperature existing prior to ignition. Conditions in the films are assumed to be symmetrical with respect to the drop center.

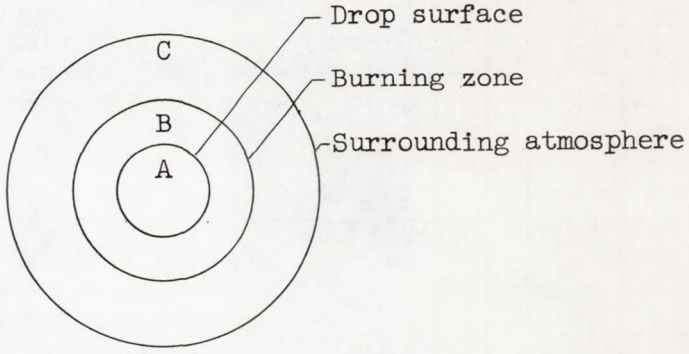

If the change in thermal conductivity with variation in composition along a radius is neglected, the heat-transfer equation (symbols are defined in appendix A) for the region between drop surface and burning zone is

$$\int_{T_A}^{T_B} \frac{k_{AB}\, dT}{L + \Delta H + h_f - h_{f_A}} = \frac{-1}{2\pi} \frac{dW_l}{dt} \left(\frac{1}{d_A} - \frac{1}{d_B} \right) \tag{B1}$$

Similarly, for the region between the burning zone and surrounding atmosphere,

$$\int_{T_C}^{T_B} \frac{k_{BC}\, dT}{Q - \left[(h_p - h_{O_2}) - (h_p - h_{O_2})_Q \right]} = \frac{-1}{2\pi} \frac{dW_l}{dt} \left(\frac{1}{d_B} - \frac{1}{d_C} \right) \tag{B2}$$

The relation for equimolal counter diffusion was used to determine the rate of diffusion of oxygen to the burning zone. For the present case (as for most hydrocarbon fuels) where the ratio of products to reactants is close to unity and for the range of oxygen concentrations investigated, this relation gives values within a few percent of those

given by the method of reference 5 or the more detailed method of reference 11. Oxygen diffusion is related to heat transfer in the region between the burning zone and surrounding atmosphere according to the following equation:

$$\int_{T_C}^{T_B} \frac{k_{BC}\, dT}{\rho D_{O_2}\left[Q - (h_p - h_{O_2}) + (h_p - h_{O_2})_C\right]} = \frac{M_{O_2}\, \alpha_C}{100\, r_{O_2}} \tag{B3}$$

From equation (B3), the burning-zone temperature T_B may be determined as a function of α_C.

If the film thickness between the burning zone and the surrounding atmosphere is considered infinite, d_C in equation (B2) becomes infinite and equations (B1) and (B2) may be combined to give

$$\frac{dW_l}{dt} = -2\pi d_A\left[\int_{T_A}^{T_B} \frac{k_{AB}\, dT}{L + \Delta H + h_f - h_{f_A}} + \int_{T_C}^{T_B} \frac{k_{BC}\, dT}{Q - \left[(h_p - h_{O_2}) - (h_p - h_{O_2})_C\right]}\right] \tag{B4}$$

Now

$$W_l = \rho_l \frac{\pi d_A^3}{6} \tag{B5}$$

When equation (B5) is differentiated and combined with equation (B4),

$$d_A d(d_A) = -\frac{4}{\rho_l}\left[\int_{T_A}^{T_B} \frac{k_{AB}\, dT}{L + \Delta H + h_f - h_{f_A}} + \int_{T_C}^{T_B} \frac{k_{BC}\, dT}{Q - \left[(h_p - h_{O_2}) - (h_p - h_{O_2})_C\right]}\right] dt \tag{B6}$$

Integrating equation (B6) over the limits

$$d_A = d_{A_0} \quad \text{when} \quad t = 0$$

and

$$d_A = d_A \quad \text{when} \quad t = t$$

yields

$$d_A^2 - d_{A_O}^2 = -\frac{8}{\rho_l}\left[\int_{T_A}^{T_B} \frac{k_{AB}\,dT}{L + \Delta H + h_f - h_{f_A}} + \int_{T_C}^{T_B} \frac{k_{BC}\,dT}{Q - \left[(h_p - h_{O_2}) - (h_p - h_{O_2})_C\right]}\right] t \tag{B7}$$

Then equation (B7) may be given as

$$d_A^2 = d_{A_O}^2 - \beta t \tag{B8}$$

where

$$\beta = \frac{8}{\rho_l}\left[\int_{T_A}^{T_B} \frac{k_{AB}\,dT}{L + \Delta H + h_f - h_{f_A}} + \int_{T_C}^{T_B} \frac{k_{BC}\,dT}{Q - \left[(h_p - h_{O_2}) - (h_p - h_{O_2})_C\right]}\right] \tag{B9}$$

Here, β, known as the evaporation constant, has the units square feet per second; for β in square microns per second, the right side of equation (B9) is multiplied by 9.3×10^{10}. For the calculation of β, the density of the isooctane drop was taken as 43 pounds per cubic foot. The drop-surface temperature was assumed to be 211° F. The temperatures of both the surrounding atmosphere and the drop prior to burning were assumed to be 77° F.

The graphical integration of the first integral of equation (B9) is shown in figure 8. The thermal conductivity k_{AB} taken as that of isooctane vapor, was calculated by assuming constant Prandtl number and calculating the temperature change in viscosity by means of the Sutherland equation ($C = 1008^\circ$ R). The thermal conductivity at a base temperature of 32° F was estimated from values given in reference 12. The enthalpy and specific heat of isooctane vapor were obtained from extrapolation of values given in reference 13.

The graphical integration of the second integral on the right side of equation (B9) is presented in figure 9. The method of reference 14 was used to determine the equilibrium composition of the diffusing products for a carbon-hydrogen-oxygen-nitrogen ratio of 8:18:25:100 over the desired temperature range. Since, at a given temperature, the effect of nitrogen on the relative proportion of dissociated products is small, the equilibrium compositions at the above ratio were used for all oxygen concentrations. This ratio was assumed to hold throughout the region

between the burning zone and the surrounding atmosphere. The products of combustion diffusing to the surrounding atmosphere were considered to consist of all equilibrium products except nitrogen. Below 2000° F, the diffusing products were considered to consist of carbon dioxide and water vapor as determined from the stoichiometric equation. The thermal conductivity k_{AB} was taken as that of air and determined from extrapolation of values given in reference 15.

A plot of the burning-zone temperature T_B against oxygen concentration in the surrounding atmosphere as determined from equation (B3) is presented in figure 10. In this integration, the ratio $k_{BC}/\rho D_{O_2}$, which was assumed to be independent of temperature, was evaluated at 77° F. The diffusion coefficient of oxygen was taken as 2.22×10^{-4} square feet per second at 77° F (ref. 16).

From figures 8 to 10 and equation (B9), the evaporation constant β may be determined as a function of the oxygen concentration α_C of the surrounding oxygen-nitrogen atmosphere.

APPENDIX C

BURNING OF LIQUID-FUEL SPRAY

In reference 3, Probert obtained an expression similar in form to the following equation for the evaporation of a liquid-fuel spray

$$100 - \eta_T = 100 \int_{\sqrt{\beta t}}^{\infty} \left(1 - \frac{\beta t}{x^2}\right)^{\frac{3}{2}} \left(\frac{-n x^{n-1}}{\bar{x}^n}\right) e^{-\left(\frac{x}{\bar{x}}\right)^n} dx \qquad (C1)$$

where η_T, the combustion efficiency, is the percent by weight of the total fuel-spray evaporated after a time t, and β is the evaporation constant for the individual drops. The expression applies for the evaporation of a spray when the evaporation rate of the individual drops is proportional to the drop diameter and when the size distribution of drops in the spray is given by the Rosin-Rammler distribution law in the form

$$R = e^{-\left(\frac{x}{\bar{x}}\right)^n} \qquad (C2)$$

where R is the fraction by weight of the initial spray consisting of drops having diameters larger than x. For a given fuel, nozzle, and fuel-flow rate, $\bar{x}$ and n are constants. In reference 3, equation (C1) was transformed and a solution was obtained by graphical integration for various values of n. The curves so obtained (fig. 11) relate η_T to $\beta t/\bar{x}^2$ for values of n ranging from 2 to 3.5.

For the case of a fuel spray burning in a duct, the average velocity of the gases at any station is a function of the combustion efficiency at that station. Consider a duct of constant cross-sectional area A and length L. Assume that the velocity of the burning drops along the duct at the station considered is given by the average velocity V of the gases at that station. For low fuel-air ratios, V can be approximated by neglecting the effects of the products of combustion on the weight flow rate, the average molecular weight, and the average specific heat of the gases.

From the continuity equation and the perfect gas law,

$$V = \frac{W}{\rho A} = \frac{WRT}{PA} \qquad (C3)$$

where W is the weight flow rate of air supplied to the duct, R is the gas constant, and P, ρ and T are the pressure, average density and average temperature of the air, respectively, at the station considered. For negligible pressure drop along the combustor,

$$P = P_i \tag{C4}$$

where P_i is the inlet pressure. If a constant specific heat c_p is assumed,

$$T = T_i + \frac{fH\,\eta_T}{100c_p} \tag{C5}$$

where T_i is the inlet-air temperature, f is the over-all fuel-air ratio, and H is the lower heating value of the fuel.

Substituting equations (C4) and (C5) into equation (C3) and rearranging yield

$$V = \frac{WRT_i}{P_i A}\left(1 + \frac{fH\,\eta_T}{100c_p\,T_i}\right)$$

$$V = V_r\left(1 + \frac{fH\,\eta_T}{100c_p\,T_i}\right) \tag{C6}$$

where V_r is the inlet-air velocity.

At the station considered

$$ds = Vdt \tag{C7}$$

where ds is the distance the fuel spray moves along the duct in the time dt. Since β and $\bar{x}^{-2}$ are constant along the duct, equation (C7) may be written

$$ds = \frac{V\bar{x}^{-2}}{\beta}\,d\left(\frac{\beta t}{\bar{x}^{-2}}\right) \tag{C8}$$

Substituting equation (C6) into equation (C8) and rearranging yield

$$\frac{\beta}{\bar{x}^{-2}\,V_r}\,ds = d\left(\frac{\beta t}{\bar{x}^{-2}}\right) + \frac{fH\,\eta_T}{100c_p\,T_i}\,d\left(\frac{\beta t}{\bar{x}^{-2}}\right) \tag{C9}$$

The boundary conditions are

(a) at $s = 0$, $\eta_T = 0$, $\frac{\beta t}{\overline{x}^2} = 0$

(b) at $s = L$, $\eta_T = \eta_T$, $\frac{\beta t}{\overline{x}^2} = \left(\frac{\beta t}{\overline{x}^2}\right)_{\eta_T}$

Integrating equation (C9) over the duct for these boundary conditions produces

$$\frac{\beta}{\overline{x}^2 V_r}\int_0^L ds = \int_0^{\left(\frac{\beta t}{\overline{x}^2}\right)_{\eta_T}} d\left(\frac{\beta t}{\overline{x}^2}\right) + \frac{fH}{100 c_p T_i}\int_0^{\left(\frac{\beta t}{\overline{x}^2}\right)_{\eta_T}} \eta_T d\left(\frac{\beta t}{\overline{x}^2}\right)$$

$$\frac{\beta L}{\overline{x}^2 V_r} = \left(\frac{\beta t}{\overline{x}^2}\right)_{\eta_T} + \frac{fH}{100 c_p T_i}\int_0^{\left(\frac{\beta t}{\overline{x}^2}\right)_{\eta_T}} \eta_T d\left(\frac{\beta t}{\overline{x}^2}\right) \qquad \text{(C10)}$$

The first term on the right side of equation (C10) represents the value of $\beta t/\overline{x}^2$ corresponding to the given values of η_T and n from figure 11. The integral in the second term is given by the area under the curve in figure 11 for the given value of n from $\beta t/\overline{x}^2 = 0$ to the value of $\beta t/\overline{x}^2$ corresponding to the given value of η_T. In figure 12, the integral is plotted against η_T for the values of n used in figure 11. For a combustor of varying cross-sectional area, the actual length L is replaced by an equivalent length $L_{eq} = KL$ where the value of K will depend on the combustor geometry.

From figures 11 and 12, equation (C10), and the values of $\overline{x}$ and n for the given fuel spray, curves of η_T against $\beta L/V_r$ can be prepared for desired values of $fH/100c_p T_i$. In figure 6, curves of η_T against $\beta L_{eq}/V_r$ are presented for the values of $\overline{x}$ obtained for the conditions of the present investigation. Since n has a small effect on the theoretical combustion efficiency and since the values of n for the fuel spray varied over a narrow range about 2.5, the curves of figure 6 were obtained for $n = 2.5$. The values of $fH/100c_p T_i$ were calculated for $T_i = 500^\circ$ R, $c_p = 0.25$ Btu per pound per $^\circ$R, and $H = 19{,}065$ Btu per pound. The values of f were based on an inlet oxygen-nitrogen mixture flow of 1.0 pound per second and nominal fuel-flow rates of 0.0157 and 0.010 pound per second.

REFERENCES

1. Graves, Charles C.: Effect of Oxygen Concentration of the Inlet Oxygen-Nitrogen Mixture on the Combustion Efficiency of a Single J33 Turbojet Combustor. NACA RM E52F13, 1952.

2. Graves, Charles C.: Effect of Inlet Oxygen Concentration on Combustion Efficiency of J33 Single Combustor Operating with Gaseous Propane. NACA RM E53A27, 1953.

3. Probert, R. P.: The Influence of Spray Particle Size and Distribution in the Combustion of Oil Droplets. Phil. Mag., vol. 37, no. 265, Feb. 1946, pp. 94-105.

4. Spalding, D. B.: Combustion of Liquid Fuel in a Gas Stream - I. Fuel, vol. XXIX, no. 1, Jan. 1950, pp. 2-7; cont., Part II, Fuel, vol. XXIX, no. 2, 1950, pp. 25-32.

5. Spalding, D. B.: Combustion of Fuel Particles. Fuel, vol. XXX, no. 6, June 1951, pp. 121-130.

6. Godsave, G. A. E.: The Burning of Single Drops of Fuel. Part II. Experimental Results. Rep. No. R.87, British N.G.T.E. Aug. 1951.

7. Bowes, I. G., and Joyce, J. R.: The Effects of Cone Angle, Pressure and Flow Number on the Particle Size of a Pressure Jet Atomiser. Tech. Rep. No. I.C.T./17, The Shell Petroleum Co. Ltd. (London), Mar. 15, 1948.

8. Hall, A. R., and Diederichsen, J.: An Experimental Study of the Burning of Single Drops of Fuel in Air at Pressures up to Twenty Atmospheres. Paper No. 21, Abstracts of Papers, Fourth Symposium on Combustion, M.I.T., Sept. 1-5, 1952.

9. McCafferty, Richard J.: Effect of Fuels and Fuel-Nozzle Characteristics on Performance of an Annular Combustor at Simulated Altitude Conditions. NACA RM E8C02a, 1948.

10. Dittrich, Ralph T.: Effects of Fuel-Nozzle Carbon Deposition on Combustion Efficiency of Single Tubular-Type, Reverse-Flow, Turbojet Combustor at Simulated Altitude Conditions. NACA TN 1618, 1948.

11. Wilke, C. R.: Diffusional Properties of Multicomponent Gases. Chem. Eng. Prog., vol. 46, no. 2, Feb. 1950, pp. 95-104.

12. Maxwell, J. B.: Data Book on Hydrocarbons. D. Van Nostrand and Co., Inc., 1950.

13. Souders, Mott, Jr., Matthews, C. S., and Hurd, C. O.: Relationship of Thermodynamic Properties to Molecular Structure - Heat Capacities and Heat Contents of Hydrocarbon Vapors. Ind. and Eng. Chem., vol. 41, no. 5, May 1949, pp. 1037-1048.

14. Huff, Vearl N., Gordon, Sanford, and Morrell, Virginia E.: General Method and Thermodynamic Tables for Computation of Equilibrium Composition and Temperature of Chemical Reactions. NACA Rep. 1037, 1951. (Supersedes NACA TN's 2113 and 2161.)

15. Glassman, Irvin, and Bonilla, Charles F.: The Thermal Conductivity and Prandtl Number of Air at High Temperatures. Preprint of papers for Heat Transfer Symposium, Am. Inst. Chem. Eng., Dec. 5, 1951.

16. Perry, John H.: Chemical Engineers' Handbook. Third Edition, McGraw-Hill Book Co., Inc., 1950.

TABLE I. - EVAPORATION CONSTANT β IN SQUARE MICRONS PER SECOND

Oxygen concentration in oxygen-nitrogen atmosphere, percent by volume			
17.0	20.9	24.9	34.9
1.07×10^{6}	1.12×10^{6}	1.30×10^{6}	1.40×10^{6}
1.02	1.21	1.27	1.48
1.06	1.13	1.26	1.39
1.02	1.18	1.23	1.36
1.03	1.15	1.26	1.40
1.07	1.15	1.20	1.50
1.12	1.10	1.25	1.48
1.10	1.16	1.21	1.40
1.09	1.21	1.26	1.44
1.04	1.14		
1.12	1.14		
1.10	1.15		
1.09			
$^{a}1.07 \times 10^{6}$	$^{a}1.14 \times 10^{6}$	$^{a}1.25 \times 10^{6}$	$^{a}1.43 \times 10^{6}$

[a]Arithmetic mean value of evaporation constant.

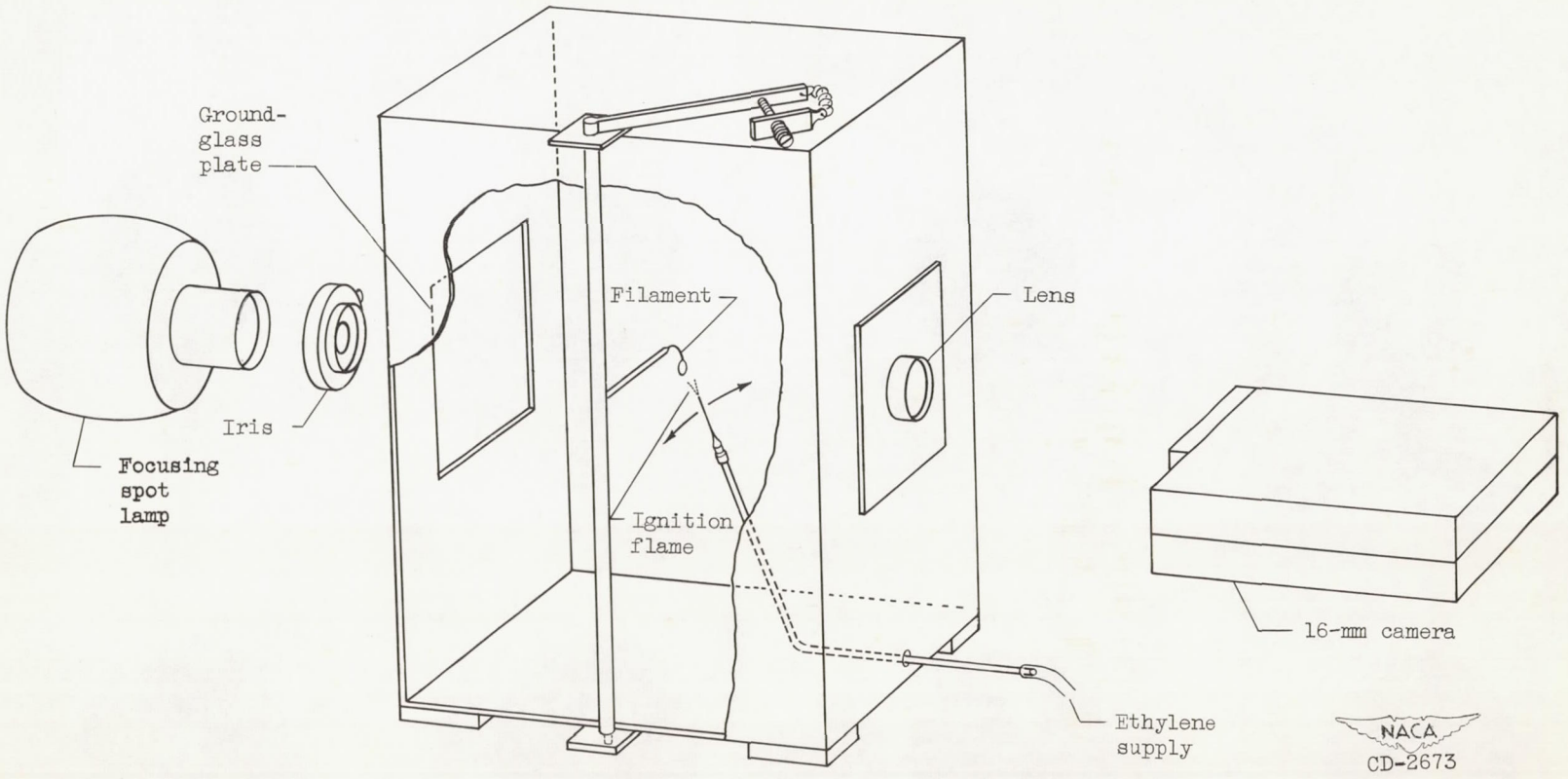

Figure 1 - Droplet burning apparatus.

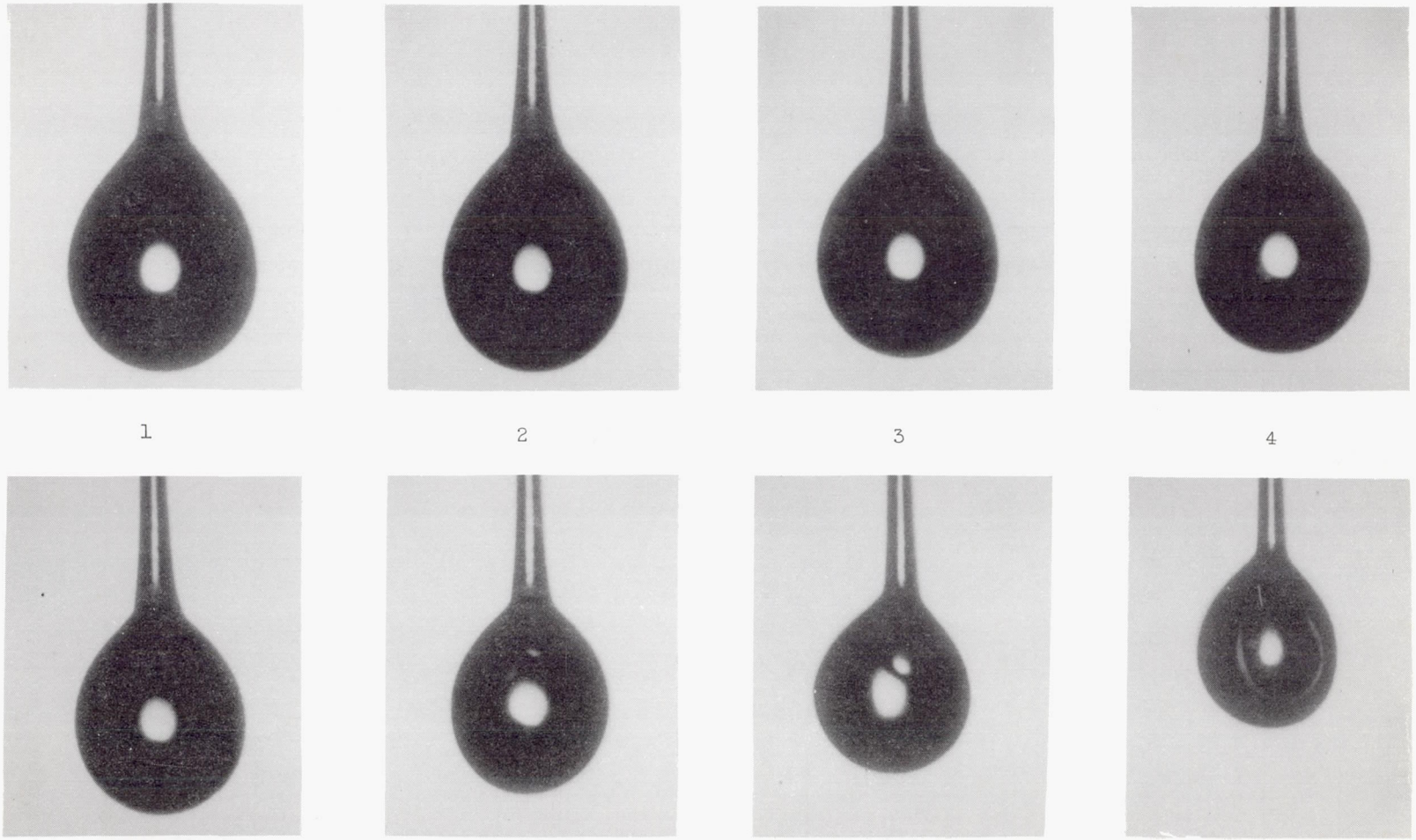

Figure 2. - Photographs of burning drop taken at intervals of 0.125 second.

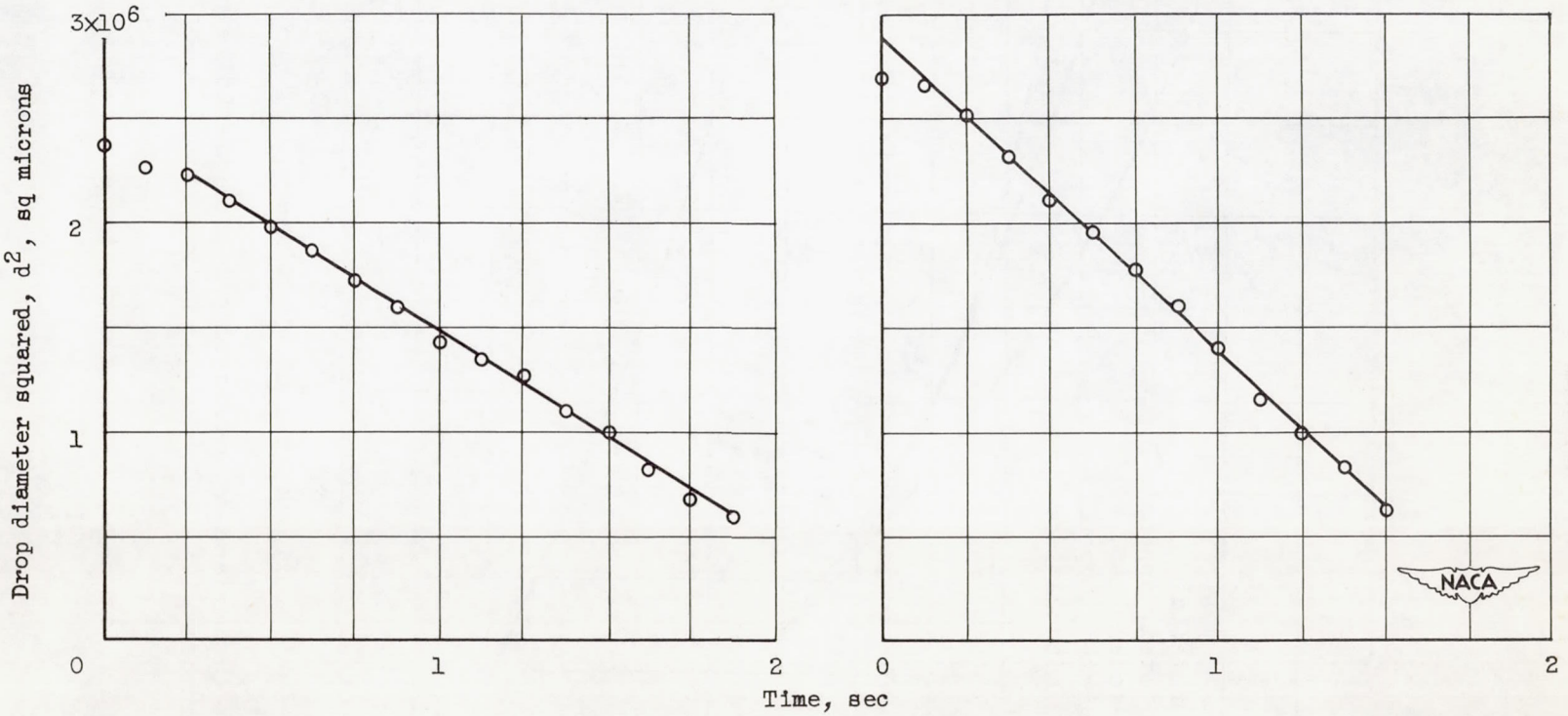

(a) Oxygen concentration, 17.0 percent by volume; evaporation constant, 1.02×10^6 square microns per second.

(b) Oxygen concentration, 34.9 percent by volume; evaporation constant, 1.50×10^6 square microns per second.

Figure 3. - Time variation in diameter of drop burning in quiescent oxygen-nitrogen atmosphere.

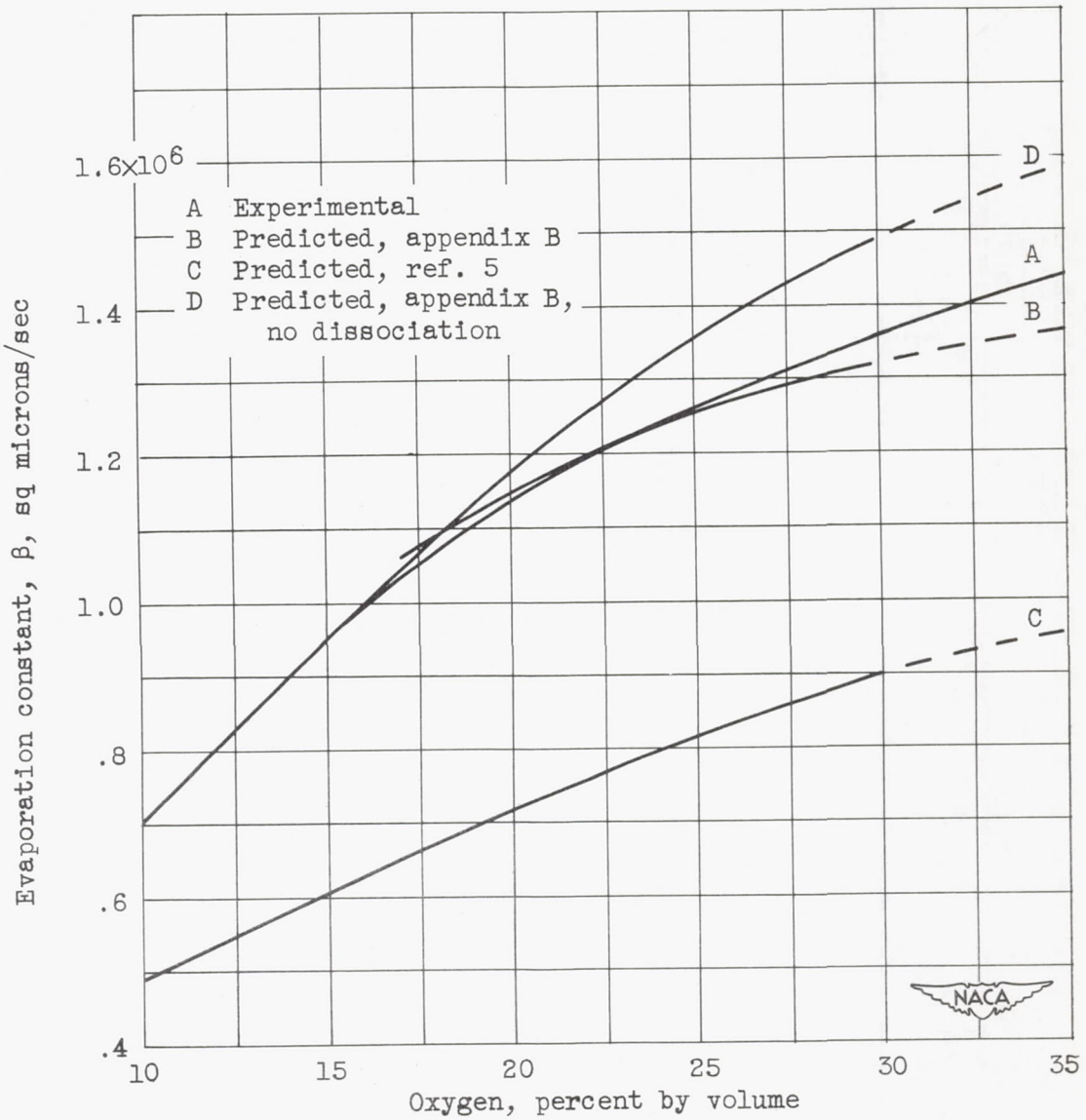

Figure 4. - Comparison of predicted and experimental evaporation constants.

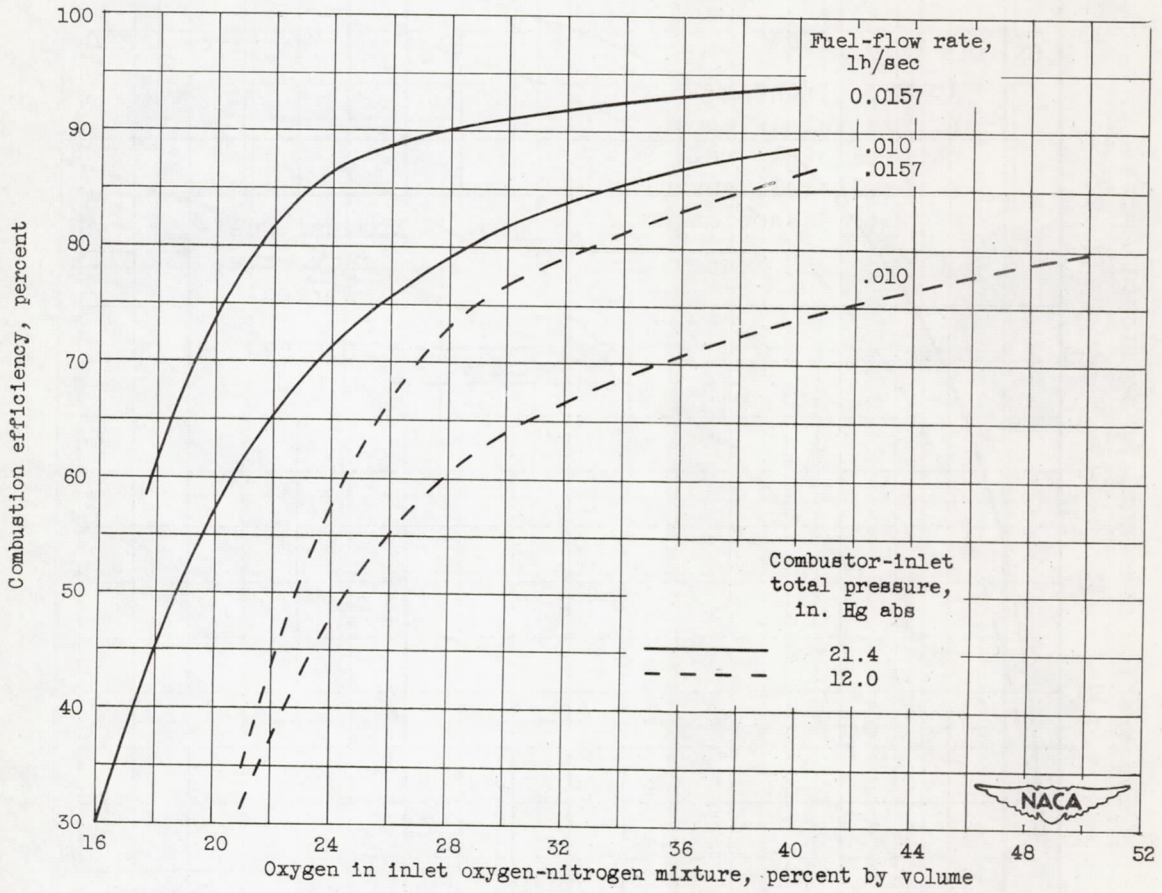

Figure 5. - Effect of inlet oxygen concentration on combustion efficiency of J33 single combustor. Fuel, isooctane; inlet temperature, 40° F; weight-flow rate of inlet oxygen-nitrogen mixture, 1.0 pound per second.

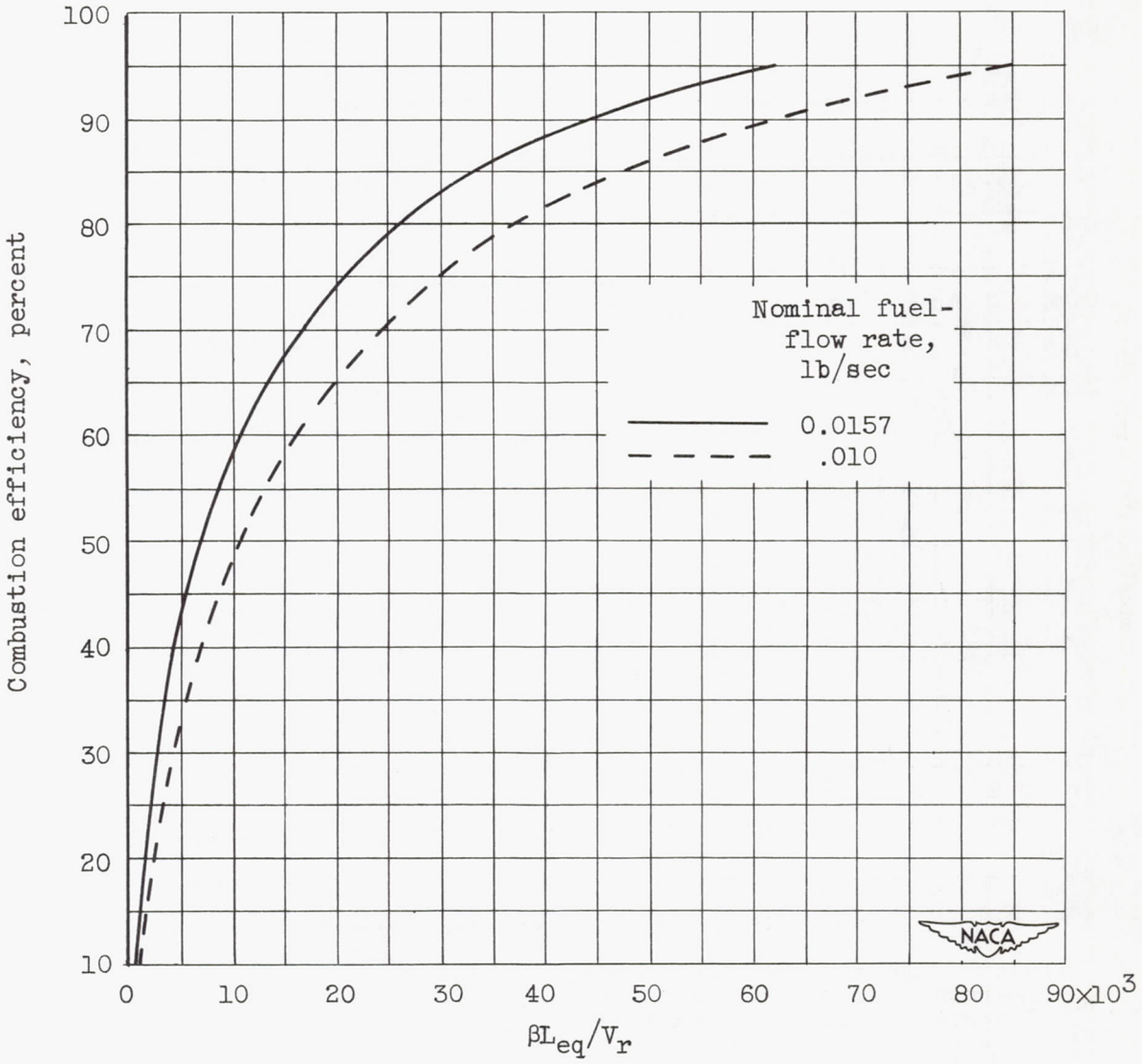

Figure 6. - Theoretical combustion efficiency of burning fuel spray. n = 2.5.

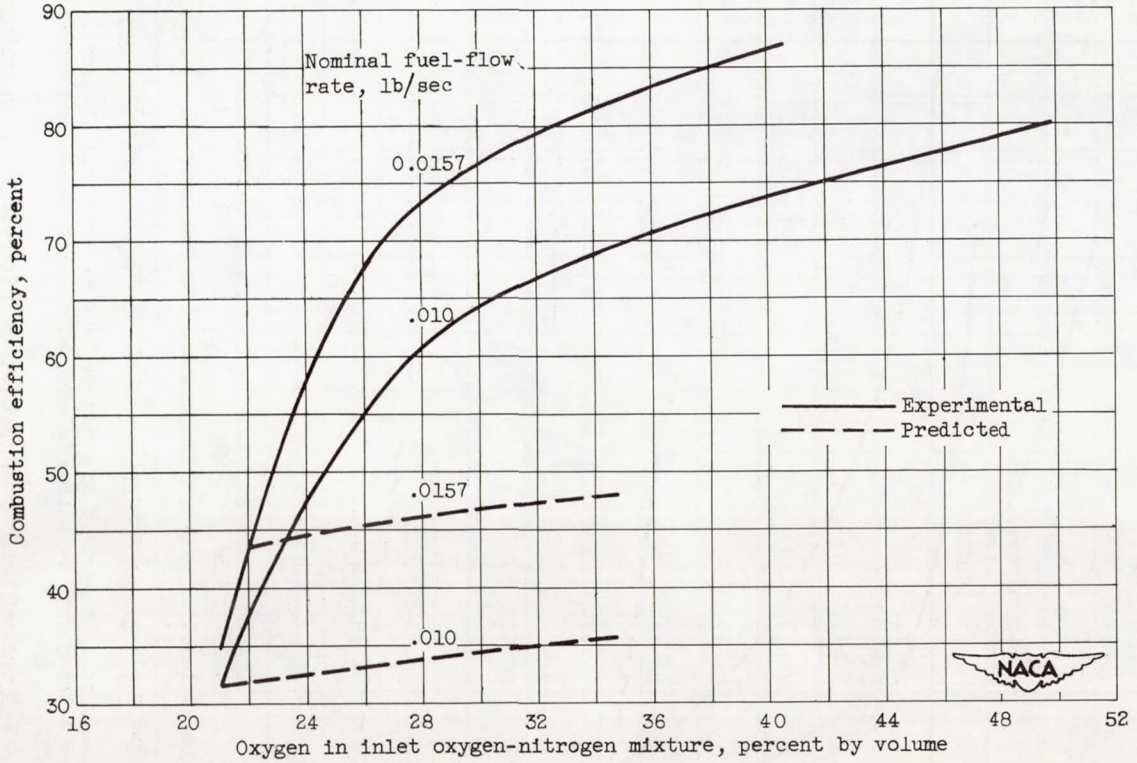

(a) Combustor-inlet pressure, 12.0 inches of mercury absolute.

Figure 7. - Comparison of predicted and experimental changes in combustion efficiency with variation in combustor-inlet oxygen concentration.

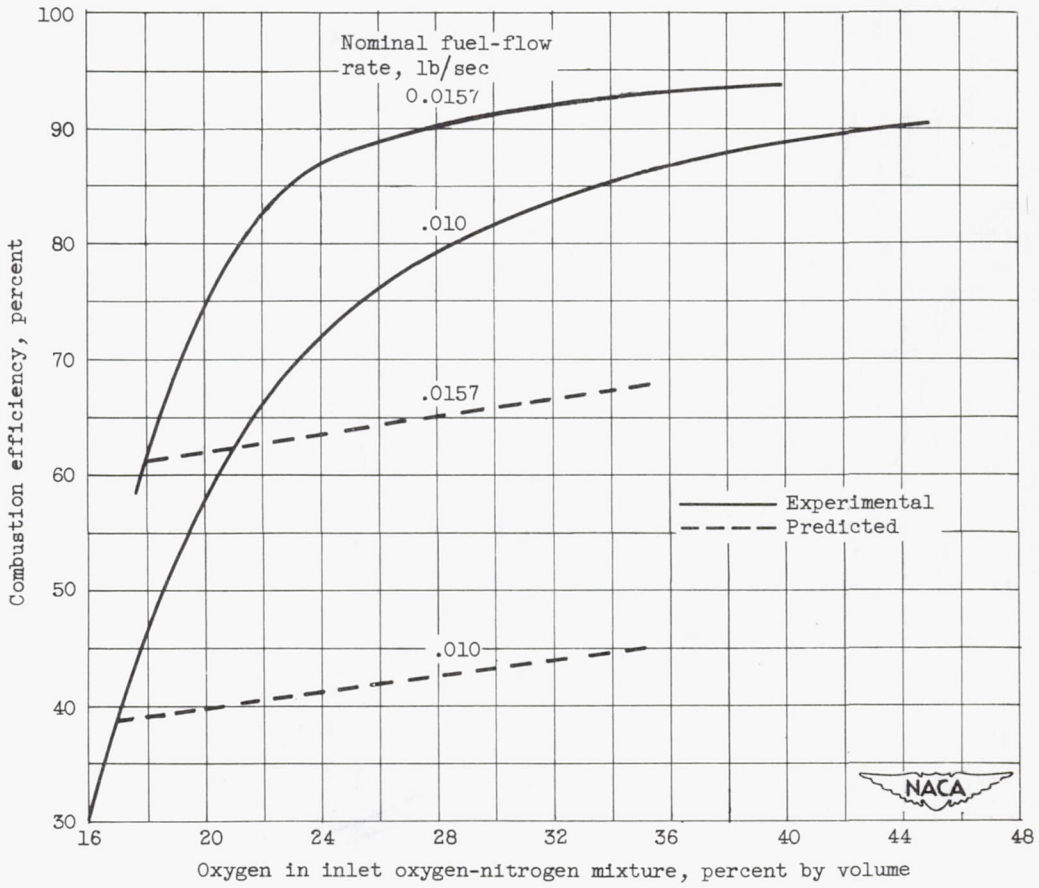

(b) Combustor-inlet pressure, 21.4 inches of mercury absolute.

Figure 7. - Concluded. Comparison of predicted and experimental changes in combustion efficiency with variation in combustor-inlet oxygen concentration.

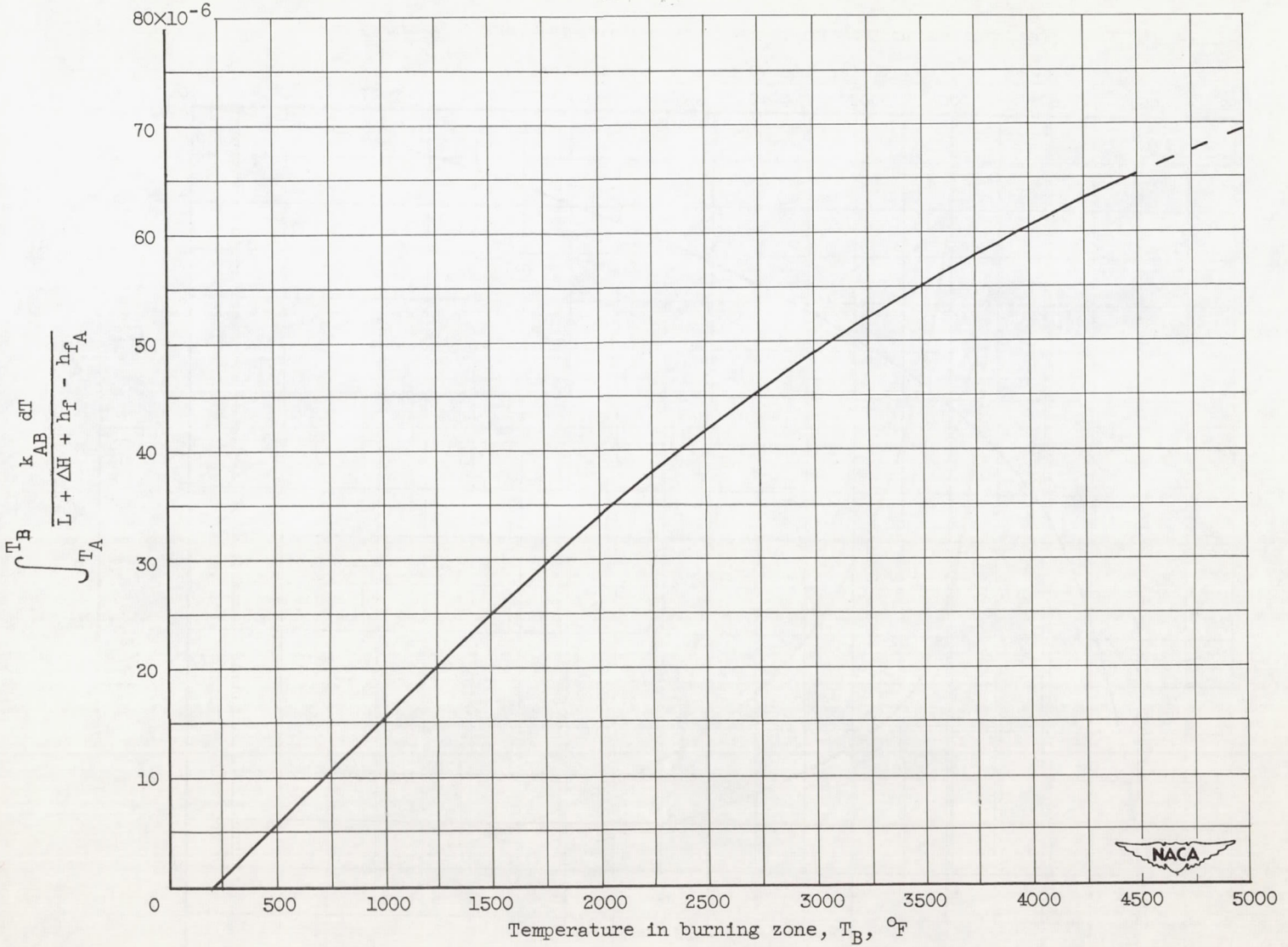

Figure 8. - Graphical integration of first integral in equation (B9).

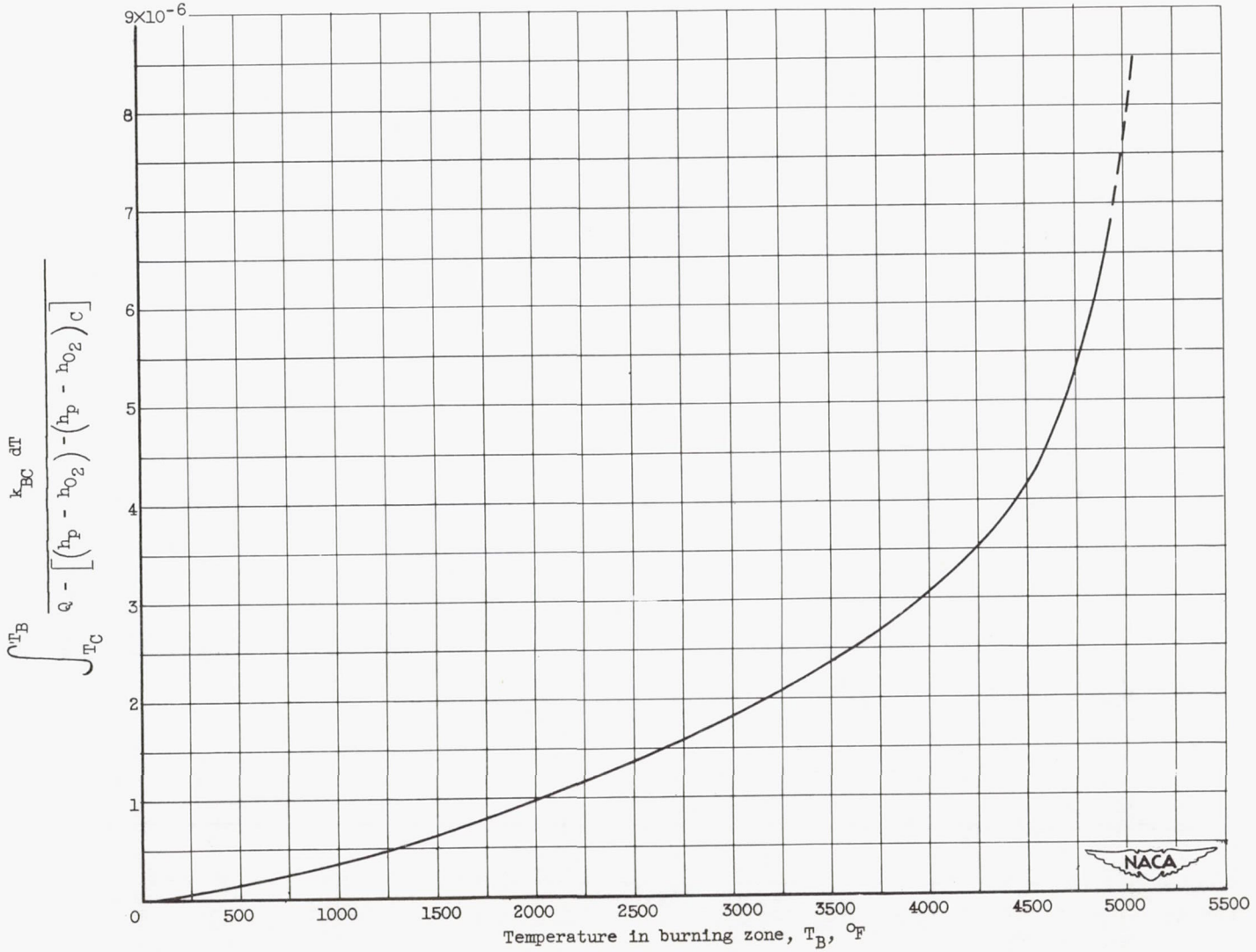

Figure 9. - Graphical integration of second integral in equation (B9).

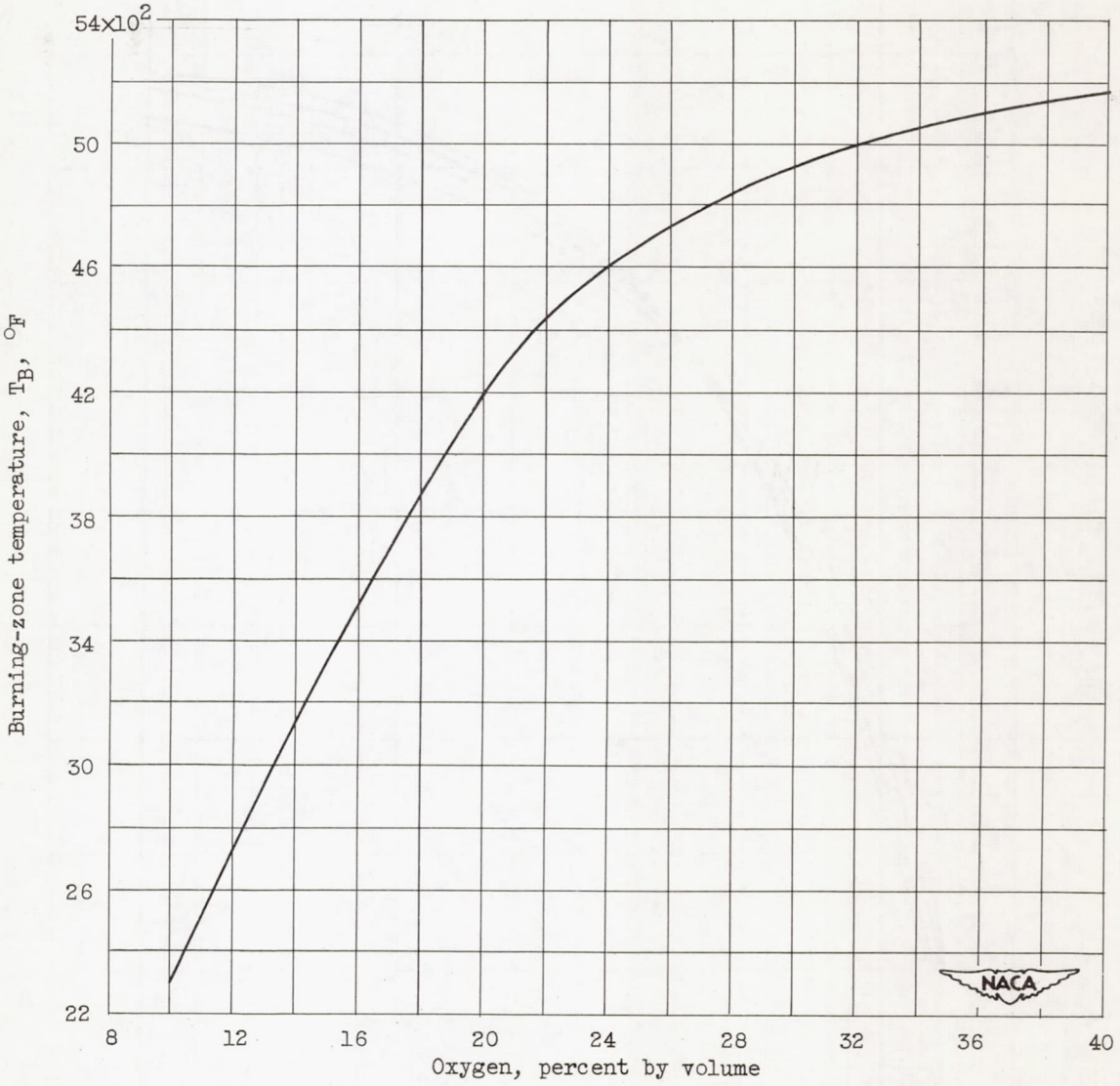

Figure 10. - Effect of oxygen concentration on burning-zone temperature.

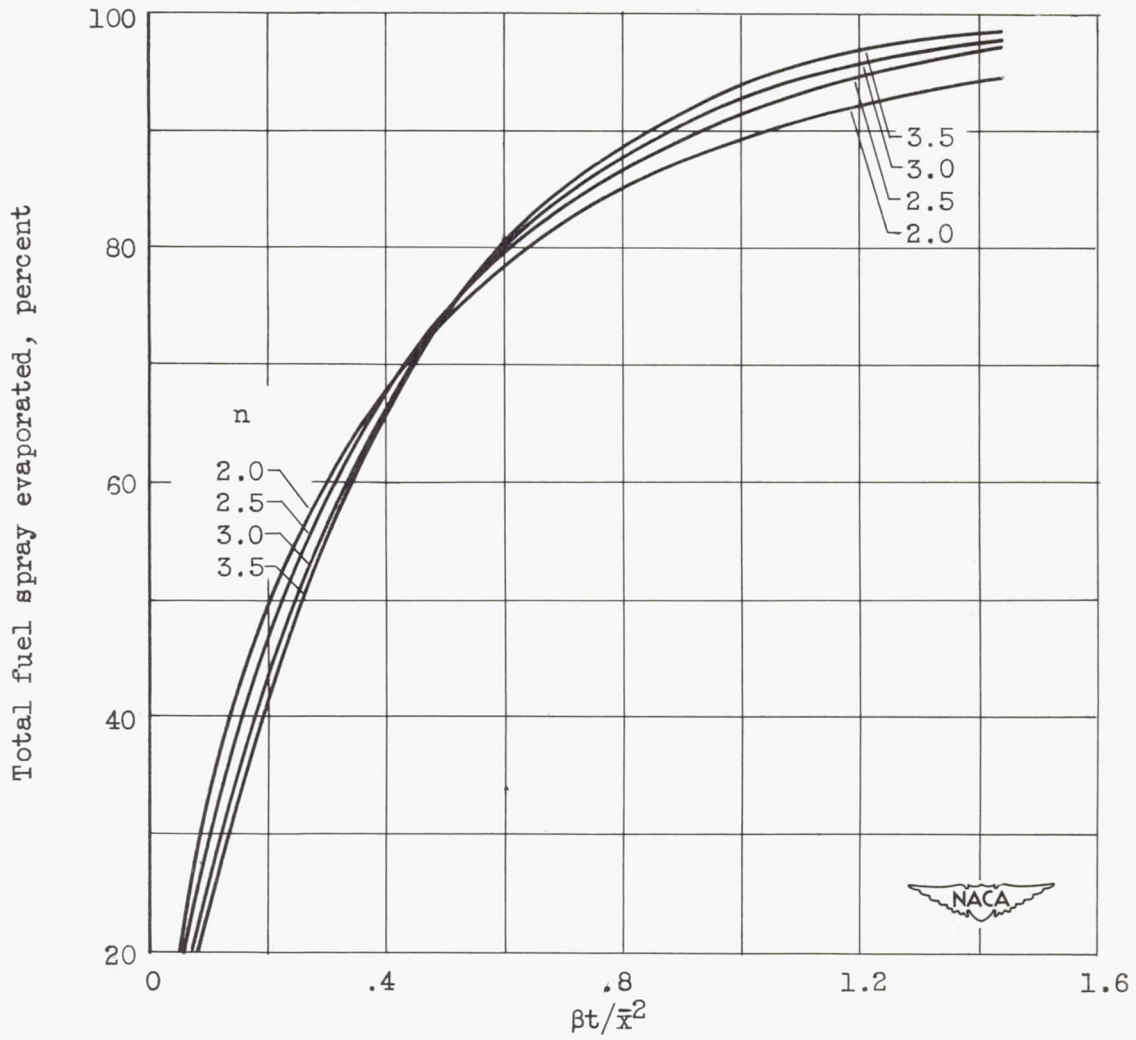

Figure 11. - Theoretical evaporation of liquid spray.

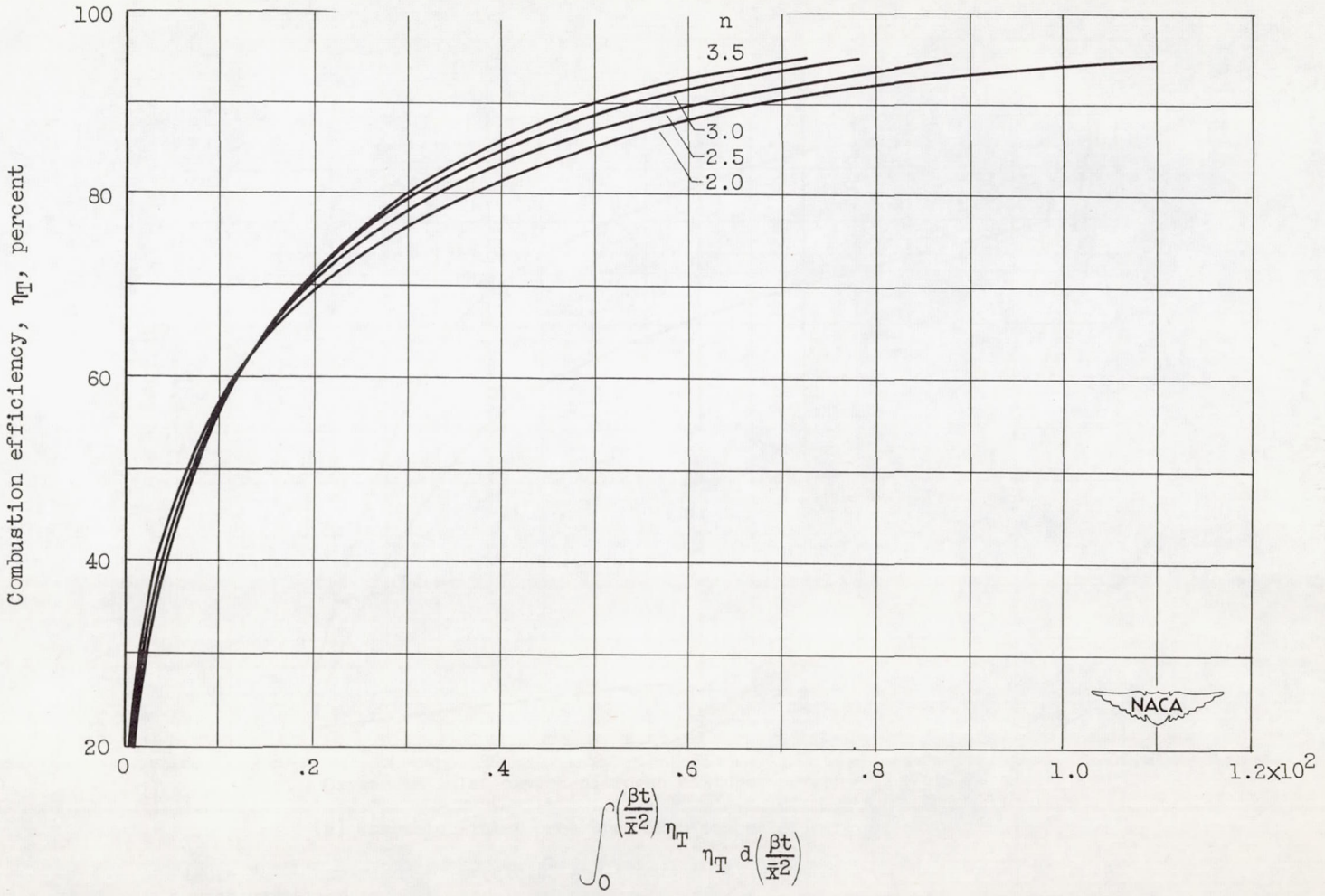

Figure 12. - Relation between $\int_0^{\left(\frac{\beta t}{\bar{x}^2}\right)} \eta_T \, d\left(\frac{\beta t}{\bar{x}^2}\right)$ and combustion efficiency.